

Anti-Corrosion Methods and Materials

Corrosion protection and mechanical performance of SiO₂ films deposited via PECVD on OT59 brass

Giuseppe Moretti

Department of Chemistry, Cá Foscari Venice University, Venice, Italy

Francesca Guidi

Department of Chemistry, Cá Foscari Venice University, Venice, Italy

Roberto Canton

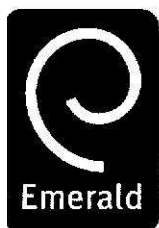
MOMA srl, Reggio Emilia, Italy

Marino Battagliarin

CNR-IENI, Corso Stati Uniti, Padua, Italy

Gilberto Rossetto

CNR-ICIS, Corso Stati Uniti, Padua, Italy



Anti-Corrosion Methods and Materials

ISSN 0003-5599

©2005 Emerald Group Publishing Limited

Editor Dr William Cox

Director, Corrosion Management,
Cheshire, UK

Assistant Editor Dr Andrew Hancock

Technical Director, Nanojet Ink Ltd,
UK

E-mail: ahancock@emeraldinsight.com

Editorial Assistant

Jessica R. Mytum-Smithson

E-mail: jmytum@emeraldinsight.com

Book Review Editor Dr Kalliopi Aligizaki

Center for Advanced Materials,
Pennsylvania State University, USA

Editorial Advisory Board

Dr Kalliopi Aligizaki

Research and Consulting Engineer,
Aedificat Institute Freiburg, Germany

Dr Peter Angell

Microbial Corrosion and Biofouling, Atomic
Energy of Canada Ltd, Chalk River, Ontario,
Canada

Dr Bui Thi An

National Centre for Scientific Research of
Vietnam, Tropical Technology Institute,
Hanoi, Vietnam

Dr Tony Betts

Corrosion Section, CREST DIT, Enterprise Ireland,
Ireland

Dr C. Carfagna

Department of Materials and Production
Engineering, University of Naples, Italy

Professor E.S. Dwarakadasa

Department of Metallurgy, Indian Institute of
Science, Bangalore, India

Professor Michael L. Free

Department of Metallurgical Engineering,
University of Utah, USA

Dr Shiwei William Guan

Bredero Shaw - A ShawCor Company,
Toronto, Canada

Dr M. Brian Ives

W.W. Smeltzer Corrosion Laboratory,
McMaster University, Ontario, Canada

Dr Andrea Kalendova

Assistant Professor, Institute of Polymers,
Faculty of Chemical Technology, Czech Republic

Dr Steve Mabbutt

Power Generation and Technology Centre,
School of Industrial and Manufacturing Science,
Cranfield University, Cranfield, UK

Dr M. Okada

National Research Institute for Metals, Nuclear
Materials Division, Tsukuba Laboratories,
Ibaraki, Japan

Dr A. Oni

Department of Metallurgical and Materials
Engineering, Federal University of Technology,
Ondo State, Nigeria

Dr Steven Percival

Microbiology Research Group, Department of
Biological Sciences, University College Chester,
Chester, UK

Dr Chris Ringas

Pipeline Performance Technologies (Pty) Ltd,
Johannesburg, South Africa

Dr C.J.E. Smith

Chief, Corrosion and Protection, Structural
Materials Centre, DRA, Farnborough, UK

Professor S. Ray Taylor

Division of Biomaterials, University of
Mississippi Medical Center, USA

Professor G.E. Thompson

Corrosion and Protection Centre, UMIST,
Manchester, UK

Dr G.M. Tsangaris

Materials Science and Engineering, National
Technical University, Athens, Greece

Anti-Corrosion Methods and Materials provides a broad coverage of the materials and techniques employed in corrosion prevention. Coverage is essentially of a practical nature and designed to be of material benefit to those working in the field. Proven applications are covered together with company news and new product information. *Anti-Corrosion Methods and Materials* now also includes research articles that reflect the most interesting and strategically important research and development activities from around the world. A review process involving the editor and other subject experts ensures the content's validity and relevance.



Certificate number ...176879...

Awarded in recognition of Emerald's production department's adherence to quality systems and processes when preparing scholarly journals for print

Dr James T. Walker

Pathogen Microbiology Group, CAMR,
Salisbury, UK

Dr Fuhui Wang

State Key Laboratory for Corrosion and
Protection, Institute of Metal Research, Chinese
Academy of Sciences, Shenyang, China

Dr Graham A. Wright

Chemistry Department, The University of
Auckland, New Zealand

Managing Editor Vicky Williams

Produced by Alden Multimedia,
Northampton

Indexed and abstracted in:

AMF Alert (Australian Mineral Foundation)
API Technical Literature Abstracts: (Electronic
Database)

API Technical Literature Abstracts:

Catalysts/Zeolites

API Technical Literature Abstracts: Fuel

Reformation

API Technical Literature Abstracts: Health &

Environment

API Technical Literature Abstracts: Oil Field

Chemicals

API Technical Literature Abstracts: Petroleum

Refining & Petrochemicals

API Technical Literature Abstracts: Petroleum

Substitutes

API Technical Literature Abstracts:

Transportation & Storage

API Technical Literature Abstracts: Tribology

Chemical Abstracts

Chemical Engineering and Biotechnology

Abstracts

Compendex Plus

CPI Digest

CSA Abstracts in New Technologies and

Engineering (ANTE)

CSA ASFA-2: Ocean Technology, Policy &

Non Living Resources Abstracts

CSA Health & Safety Science Abstracts

CSA Mechanical & Transport Engineering

Abstracts (Selective)

Engineering Index

Fluid Abstracts

Fluidex

(ISI) Alerting Services®

(ISI) Materials Science Citation Index®

(ISI) Metallurgy and Metallurgical Engineering

Citation Index®

(ISI) SciSearch®: Science Citation Index

Expanded

Scopus

World Surface Coatings Abstracts

zetoc

This journal is also available
online at
www.emeraldinsight.com/acmm.htm

Internet services available
worldwide at
www.emeraldinsight.com

Emerald Group Publishing Limited

60/62 Toller Lane,
Bradford BD8 9BY,
United Kingdom



INVESTOR IN PEOPLE

Tel +44 (0) 1274 777700

Fax +44 (0) 1274 785200

E-mail help@emeraldinsight.com

Regional offices:

For North America

Emerald, 875 Massachusetts Avenue,
7th Floor, Cambridge, MA 02139, USA
Tel Toll free +1 888 622 0075;

Fax +1 617 354 6875

E-mail america@emeraldinsight.com

For Japan

Emerald, 3-22-7 Oowada, Ichikawa-shi,
Chiba, 272-0025, Japan

Tel +81 47 393 7322;

Fax +81 47 393 7323

E-mail japan@emeraldinsight.com

For Asia Pacific

Emerald, 7-2, 7th Floor, Menara KLH,
Bandar Puchong Jaya, 47100 Puchong,
Selangor, Malaysia

Tel +60 3 8076 6009;

Fax +60 3 8076 6007

E-mail asiapacific@emeraldinsight.com

Customer helpdesk:

Tel +44 (0) 1274 785278;

Fax +44 (0) 1274 785204;

E-mail support@emeraldinsight.com

Web www.emeraldinsight.com/customercharter

Orders, subscription and missing claims enquiries:

Tel +44 (0) 1274 777700;

Fax +44 (0) 1274 785200

Missing issue claims will be fulfilled if
claimed within four months of date of
despatch. Maximum of one claim per
issue.

Reprints and permissions service:

Anne-Marie Thorslund

Tel +44 (0) 1274 785139

E-mail athorslund@emeraldinsight.com

Web www.emeraldinsight.com/reprints

www.emeraldinsight.com/permissions

No part of this journal may be reproduced,
stored in a retrieval system, transmitted in any
form or by any means electronic, mechanical,
photocopying, recording or otherwise without
either the prior written permission of the
publisher or a licence permitting restricted
copying issued in the UK by The Copyright
Licensing Agency and in the USA by The
Copyright Clearance Center. No responsibility is
accepted for the accuracy of information
contained in the text, illustrations or
advertisements. The opinions expressed in the
articles are not necessarily those of the Editor
or the publisher.

Emerald is a trading name of Emerald Group Publishing Limited

Printed by Printheus Group Ltd, Scirocco Close,
Moulton Park, Northampton NN3 6HE

Corrosion protection and mechanical performance of SiO₂ films deposited via PECVD on OT59 brass

Giuseppe Moretti and Francesca Guidi

Department of Chemistry, Ca' Foscari Venice University, Venice, Italy

Roberto Canton

MOMA srl, Reggio Emilia, Italy

Marino Battagliarin

CNR-IENI, Corso Stati Uniti, Padua, Italy, and

Gilberto Rossetto

CNR-ICIS, Corso Stati Uniti, Padua, Italy

Abstract

Purpose – To evaluate the corrosion performance and nano-mechanical behaviour of a brass substrate covered by different thick SiO₂ layers deposited by means of plasma enhanced chemical vapour deposition (PECVD) technique.

Design/methodology/approach – The comparison between laboratory and “industrial” objects revealed a very good corrosion behaviour and good mechanical performance of both of them: in particular it was possible to modulate the surface treatment to solve various problems from the industrial point of view.

Findings – It was possible to reduce the Cu migration into the SiO₂ coating during the PECVD deposition at a negligible level and to control it by the deposition; further, the nano-indentation tests revealed the great utility of the coating annealing in obtaining a significant improvement of the mechanical properties of the coated objects.

Research limitations/implications – Even if some industrial problems were solved (minimization of the presence of the coating defects and transparency of the coatings), some on the layer hardness (anti-wear behaviour of the industrial objects) has to be better investigated and possibly solved.

Practical implications – The work reports a deposition process that is carried out industrially over a two year period.

Originality/value – This research reports a PECVD process realized on industrial objects: the originality is in the reached corrosion and mechanical performances that made it possible to realize a satisfactory industrial deposition.

Keywords Corrosion protection, Brass, Films (states of matter), Substrates

Paper type Research paper

Introduction

The plasma enhanced chemical vapour deposition (PECVD) is now a technique normally used in industry in many applications, for example as optics (Tien *et al.*, 1972; Choi *et al.*, 2000), corrosion protection layers (Okuara and White, 1987; Schreiber *et al.*, 1980), and as barrier films for food packaging (Fayet *et al.*, 1995). SiO₂ dielectric films are largely employed in silicon integrated circuit technology as a passivating layer or as intermetallic insulation in multilayer structures (Sahli *et al.*, 1992; Inagaki *et al.*, 1989; Falcony

et al., 1991). Low processing temperatures make it possible to avoid segregation effects and dopant migration within the device (Selamoglou *et al.*, 1989; Patrick *et al.*, 1992).

SiO₂ layers are also used in the anti-wear and anti-corrosion field: increasing attention toward these techniques is due to the fact that now it is possible to coat large surfaces (1 m² and more), which make it increasingly attractive to industry (Sahli *et al.*, 1994; Perrin *et al.*, 2000). It has been shown that electrochemical techniques based on surface impedance measurements are very useful when controlling the integrity and quality of coatings (Kittel *et al.*, 2002; Popov *et al.*, 1993; Walter, 1991; Amirudin and Thierry, 1995; Santagata *et al.*, 1998). Studies of corrosion prevention and protection have recently reported the good correlation between electrochemical parameters and several relevant chemical-physical properties of metal surfaces, such as the water adsorption, film resistance and corrosion rate of the coated metal (Kittel *et al.*, 2002).

The Emerald Research Register for this journal is available at www.emeraldinsight.com/researchregister

The current issue and full text archive of this journal is available at www.emeraldinsight.com/0003-5599.htm



Anti-Corrosion Methods and Materials
52/5 (2005) 266–275
© Emerald Group Publishing Limited [ISSN 0003-5599]
[DOI 10.1108/00035590510615758]

This research has been supported by the Italian Ministry of University and Scientific and Technological Research (MURST).

After the deposition of very thin, transparent, homogeneous and amorphous SiO₂ films by means of hexamethyldisiloxane (HMDSO) (which provides the best results as a reagent precursor (Yasuda, 1987)), the metallic substrate rarely comes into contact with even the most aggressive external environment, therein assuring high resistance to the corrosive attack. The diffusion of aggressive species through the coating to the metal/coating interface is minimised.

From a physical standpoint, an inorganic coating with high corrosion protection efficiency can be thought of as being an electrically insulating barrier that, by preventing the contact of electrochemically active species with the metal surface, hinders the occurrence of corrosion processes. The "impermeability" of the protective coating depends on:

- 1 its thickness;
- 2 the absence of defects; and
- 3 the adhesion of the layer to the substrate.

A coating without mechanical defects, such as micro-porosity, localised cracks or poor local adhesion to the substrate metal, is obtained by tuning the layer deposition process, and, especially, by the pre-treatment, the importance of which was first pointed out by Yasuda (1987).

Plasma deposited amorphous SiO₂ also can be a good candidate to improve the abrasion and wear resistance of the substrate surface. For this purpose, the determination of the surface and near-surface mechanical properties of the film is important in order to evaluate the performance of the coating in service.

The nano-indentation technique is now widely used in evaluating the hardness of small volumes such as thin films, and several studies concerning micro-indentation and nano-indentation analysis of plasma-deposited SiO₂ on different substrates such as polymers (Rats *et al.*, 1999) or Herasil and borosilicate glass (Beck *et al.*, 1998) have been reported. However, no data, at the present, are known for the system SiO₂/brass.

This paper presents an evaluation of the corrosion performance and nano-mechanical behaviour of the brass substrate when covered by different thick SiO₂ layers deposited by means of the PECVD technique. Samples prepared by means of an industrial process were tested in a standard very aggressive solution (aerated 1N H₂SO₄ at 25°C - 1-168 h of it) by means of DC and AC measurements. SIMS analysis was employed to characterise the coating thickness and the homogeneity of the deposition. On the basis of the initial laboratory results, the same deposition process was used to cover some industrial objects, which were tested following ASTM protocols.

Methodology

PECVD treatment

The deposition system consisted of a 13.56 MHz radio frequency source, capacitively coupled (0-1,200 W) to a cylindrical process chamber. The precursor flow was ignited and adjusted to produce the desired pressure. After pressure was stabilised at about 0.1 mbar, the radio frequency energy was applied to the electrode at a power of 600 W. A 0.7 × 1.0 m² surface electrode was used as a sample holder. HMDSO and O₂ gases were employed.

The SiO₂ coating was deposited after an initial O₂ substrate activation to clean the surface from organic contamination

(Yasuda, 1987), to improve the adhesion and reduce the formation of defects (van Ooij *et al.*, 1995). The PECVD treatment was carried out at near room temperature (about 35°C). However, (as expected) an undesirably defined substrate/film interface results because of the use of O₂⁺ ions of relatively large energy (Barranco *et al.*, 2001).

Electrochemical measurements

The resulting coatings were electrochemically examined to determine their corrosion resistance in a very aggressive test solution (aerated 1N H₂SO₄ at 25°C). The methodologies used to investigate the corrosion behaviour of the PECVD treated samples included DC (Tafel curves) and AC (EIS) techniques.

Thermostatted double-walled (1 litre) Pyrex glass cells (Green cells) were used in the electrochemical tests. Brass discs of 11.3 mm diameter, (with a nominal composition of: Cu = 59 percent; Zn = 29 percent; Pb = 1 percent), were laser cut from plate. Each sample was mounted on a Teflon holder that left an exposed area of 0.5 cm², and was the working electrode. Before use, specimens were washed with distilled water, degreased with acetone and dried with a jet of air. The working electrode, a saturated calomel reference electrode (SCE) inside a Luggin capillary probe, and a platinum counter electrode, were placed inside the cell. All the reported potentials refer to SCE. Each test was repeated three times to verify its reproducibility.

The potentiodynamic tests were carried out as follows. Each specimen was immersed until a stable (± 2 mV) free corrosion potential (E_{corr}) was attained. At that point, the scan was started from the E_{corr} until a potential $E = (E_{\text{corr}} - \text{about } 400 \text{ mV})$ and recorded with a scanning rate of 1,000 $\mu\text{V/s}$. The specimen then was replaced and re-immersed inside the electrochemical cell in the same solution. After E_{corr} was reached, the anodic scan was started from the E_{corr} until a potential: $E = (E_{\text{corr}} + \text{about } 200 \text{ mV})$. The data were recorded by means of an SOLARTRON Model 1287 electrochemical interface. Each test was repeated three times on different specimens in three different solutions at the same concentration to verify its reproducibility. E_{corr} , i_{corr} and b_A values for each of the samples were determined by extrapolating Tafel lines using SOLARTRON Corrview software. The DC curve method has been extensively reported previously (Moretti *et al.*, 2002).

EIS measurements were usually performed at the corrosion potential of the brass substrate, by applying a ± 10 mV amplitude sinusoidal wave perturbation to the corroding system. The frequency values usually ranged from 10⁵ Hz to 10⁻² Hz, with ten frequency values per decade. At the end of each EIS measurement, potentiostatic polarization was interrupted and the working electrode was allowed to corrode freely until the next EIS measurement (the free corrosion potential, E_{corr} was determined in the meantime). The data were recorded by means of the electrochemical interface and a SOLARTRON Model 1260 frequency response analyser. The experimental data were interpolated with Solartron Zview software to model the best equivalent circuit to approximate the impedance behaviour. The physical model (discussed below and shown in the Figure 10) and the electrochemical model (shown in the Figure 11) enabled the charge transfer resistance (R_{ct}) and double-layer capacity (C_{dl}) of the corrosion reaction, as well as the pore resistance (R_{pore}) and the coating capacity (C_{coat}) to be determined.

The solution resistance (R_s), is generally negligible ($4\text{-}\Omega\text{ cm}^2$) because of the high solution conductivity.

The constant phase element (CPE) was used in place of a real capacitive value to compensate for the non-homogeneity of the surface caused by, for example, the corrosion process (Jüttner *et al.*, 1988; Growcock *et al.*, 1989).

In the equivalent circuit, a "W" indicated the Warburg diffusion element: it takes into account of the diffusion phenomena that can occur inside the coating, depending on, for example, the water uptake. In fact, all coated samples, specially that of higher thickness, presented an almost rectilinear part (at about 45°) in the EIS spectra recorded within 24 h (Kendig *et al.*, 1983).

IMS measurements

The obtained coated samples were examined by means of IMS measurements to verify their thickness and the treatment homogeneity. A custom-built instrument (Pagura *et al.*, 1992) was used to carry out the SIMS analysis. A monochromatic (6 keV, ionic current $\sim 400\text{ nA}$) O_2^+ ion beam, collimated to $50\text{ }\mu\text{m}$, was generated in a mass-filtered duoplasmatron ion gun (model DP50B, VG Fisons, UK). The magnification was set to 2,000X, except for the sample of 80 nm for which it was set to 1000X, reducing the current density of the beam to 25 percent.

A powerful mass-energy analyser (model EQS1000, Hiden, UK), with a high transmission 45° sector field energy analyser and a quadrupole mass-filter, was used in counting mode for positive-ion detection. Lens and energy analyser potentials, quadrupole electronic control units and the detection system were controlled through a Hiden HAL IV interface. Ion depth profiles were recorded for samples of interest as a function of bombardment time. Border effects were avoided by employing electronic gating: only a percentage (50 percent, considering the preliminary level of the investigation) of the rastered area contributed to the ionic signal, which was restricted to the central part of the crater. The craters produced by ion bombardment were measured with a surface profiler KLA Tencor (San Jose, CA) model P10. The surface roughness of iO_2 was measured by scanning $600\text{ }\mu\text{m}^2$ regions. Three depth-profiles were acquired for each sample, so as to estimate the reproducibility of the process and, therein, the uniformity and surface roughness of the silica layers.

Nano-indentation measurements

Nano-indentation was used to determine film hardness using Nanotest 600 instrument from Micromaterials Ltd with a Berkovich (threesided pyramidal) diamond indenter. Several peak loads for each sample in the range: 2.5-100 mN were used with the same loading and unloading rates: these were varied in proportion to the peak loads starting at a value of 0.1 mN/s for the 2.5 indentations, while common experimental conditions as initial (contact) load 0.05 mN and holding period at peak load 10 s were used for all the measurements. The indentations were repeated at least five times at each load on different regions of the sample surface, $10\text{ }\mu\text{m}$ apart. The hardness (H) and reduced modulus (E_r) have been determined from these indentation curves using a method originally proposed by Oliver, which fits a power-law function to the unloading curve (Oliver and Pharr, 1992). The nano-indentation measurements were also carried out on annealed samples: the annealing was performed in oxygen atmosphere at 500°C (1 h).

Results

Electrochemical tests – DC results

Figure 1 shows some typical " i vs E " curves (Tafel curves) obtained with different SiO_2 (from 180 to 1,950 nm thick) specimens after 1 h of immersion time in aerated 1N H_2SO_4 at 25°C , compared to the sample of untreated brass substrate. Figure 2 shows the same curves obtained with the same samples at 168 h of immersion time (1 week) in the same experimental conditions. Table I summarises the electrochemical DC results.

Figure 1 Some typical Tafel curves obtained with uncoated and SiO_2 -coated brass (in aerated 1N H_2SO_4 at 25°C ; after 1 h)

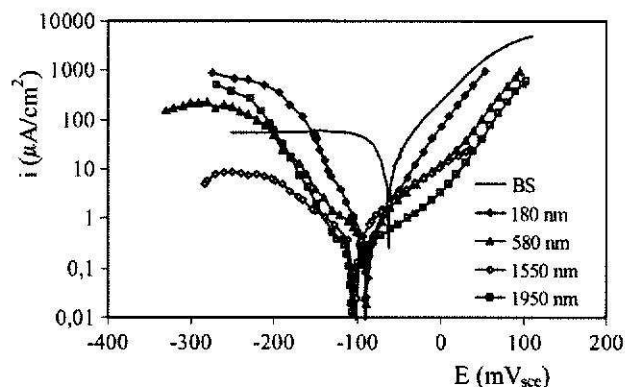


Figure 2 Some typical Tafel curves obtained with uncoated and SiO_2 -coated brass (in aerated 1N H_2SO_4 at 25°C ; after 168 h)

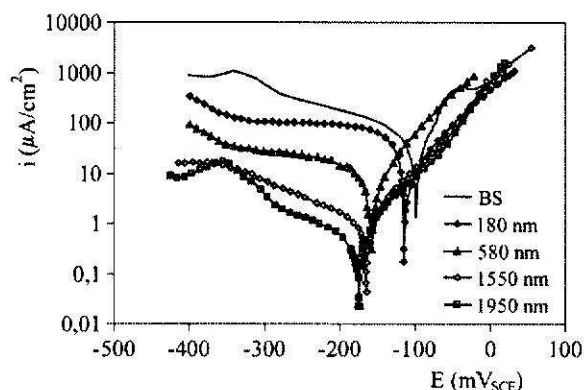


Table I Electrochemical data obtained in the DC tests

Immersion time (h)	Coating thickness (nm)	E_{corr} (mV _{SCE})	b_A (mV/dec)	i_{corr} ($\mu\text{A}/\text{cm}^2$)
1	0	-107	45	16.1
	180	-83	56	1.3
	580	-89	73	1.0
	1,550	-100	86	0.4
	1,950	-97	90	0.2
168	0	-104	31	20.2
	180	-122	72	0.5
	580	-143	70	0.3
	1,550	-155	72	0.4
	1,950	-159	72	0.3

After 1 h all the PECVD treatments influenced the corrosion current (i_{corr}) (Table I). All the curves of the treated specimens were clearly shifted to lower i_{corr} values, with respect to those of the brass substrate (Figure 1). In these experimental conditions, the i_{corr} value of the brass was about $16 \mu\text{A}/\text{cm}^2$, whereas those calculated for the different coatings were significantly lower (at least one order of magnitude), ranging from 1.3 to about $0.2 \mu\text{A}/\text{cm}^2$ (Table I). In the short term tests, the 1,950 nm thick layer reached, on average, the lowest i_{corr} , $0.2 \mu\text{A}/\text{cm}^2$, and was almost two orders of magnitude lower than that of the brass substrate.

In the short immersion tests, as the PECVD treatment time and, consequently, the thickness of the SiO_2 layer increased (Table I). The average E_{corr} values seemed not to be significantly influenced, ranging from around -90 to $-100 \text{ mV}_{\text{sce}}$.

At the end of the experiments (168 h) the various PECVD treatments behaved in a quite different way. Actually, after 168 h, the corrosion reaction mechanism seems to be almost the same for the various coatings, as evidenced by the curve shape that is very similar for the various specimens. As reported in Table I, the anodic Tafel slopes for the coated samples ranged all around $70 \text{ mV}/\text{dec}$. Thus, the E_{corr} values became as much more negative as coating thickness increased (from -113 to -174 in comparison with $-98 \text{ mV}_{\text{sce}}$ - Table I).

AC (EIS) results

The EIS results are summarised in Table II. Figures 3 and 4 show the capacitance and resistance trends over time. The charge transfer resistance (R_{ct}) and the pore resistance (R_{pore}) trends vs coating thickness were very similar in all cases (Figure 3): though higher values were found with the 1,950 nm coating thickness.

Their values increased with time to a maximum after 1-48 h and then slowly diminished reaching a stable value in 72-168 h of immersion time (Table II).

By the comparison between the double-layer capacity (C_{dl}) as well as the coating capacity (C_{coat}) values, one can note that, on average, the C_{dl} values were significantly lower than were those of C_{coat} (ranging from about 100 to $200 \mu\text{F}/\text{cm}^2$ for all thicknesses - Table II): in fact the coatings act as a substrate insulator, and even if the solution penetrated in the layer defects, the C_{coat} remained significantly higher than the C_{dl} . After 168 h of immersion time, the C_{coat} values, on average, decreased. At 168 h the minimum C_{coat} value was only reached by the 1,950 nm coating (about $1,200 \mu\text{F}/\text{cm}^2$).

SIMS results

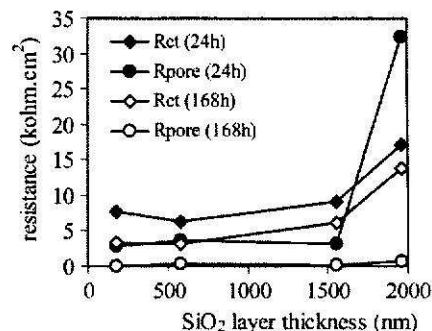
The thickness of SiO_2 layers deposited on the brass samples was measured by the SIMS technique that made it possible to obtain also the depth-profiles of the most representative elemental - or molecular - ions, associated to deposited SiO_2 , interface regions and substrate. Table III presents the thickness data obtained for the different PECVD treatments; Figures 5 and 6 show the element profiles obtained for the 180 and 1,950 nm layer thicknesses.

There was evident proportionality in the thickness of SiO_2 as a function of the PECVD treatment time. The sample exposed to plasma for only 5 min (180 nm thick) showed an uncertainty of about 40 percent, probably due to the residual roughness of the substrate and intrinsic defects in the analysis, such that due to the crater walls, generated by the technique, that are irregular and discernible with care. The resulting

Table II The EIS data obtained for the PECVD treated samples in aerated 1N H_2SO_4 . R_{ct} : charge transfer resistance; C_{dl} double-layer capacity; R_{pore} : pore resistance; C_{coat} : coating capacity

Coating thickness (nm)	Immersion time (h)	R_{ct} ($\Omega \text{ cm}^2$)	C_{dl} ($\mu\text{F}/\text{cm}^2$)	R_{pore} ($\Omega \text{ cm}^2$)	C_{coat} ($\mu\text{F}/\text{cm}^2$)
0	1	830	63		
	24	220	426		
	48	205	859		
	72	108	1,796		
	168	97	12,342		
180	1	5,450	162	2,857	12,954
	24	7,620	62	3,747	11,114
	48	5,744	283	5,449	14,213
	72	5,971	409	5,985	11,669
	168	3,350	952	651	43,292
580	1	4,207	109	3,699	196
	24	6,280	85	4,207	3,152
	48	6,351	170	4,850	33,198
	72	6,199	208	5,400	37,205
	168	3,110	1,606	300	1,955
1,550	1	1,950	62	3,220	3,567
	24	9,098	266	3,240	1,047
	48	3,058	358	3,254	1,243
	72	2,554	457	2,238	1,476
	168	6,090	742	260	2,152
1,950	1	19,902	249	9,281	63
	24	17,129	221	32,392	59
	48	24,212	203	28,786	181
	72	20,472	160	22,530	267
	168	13,883	358	676	1,217

Figure 3 R_{ct} and R_{pore} trends vs the layer thickness in aerated 1N H_2SO_4 (25°C) at 1 and 168 h of immersion time



thickness was obtained considering the maximum intensity of the $^{11}\text{B}^+$ signal as an indicator of the silica-brass interface.

When the PECVD treatment was carried out to reach 1,550 or 1,950 nm of coating thickness (for 30 and 45 min, respectively), Cu migrated in the SiO_2 layer during the deposition: for the 1,950 nm specimen, for example, the Cu started to migrate from the brass surface into the coating (up to $1 \mu\text{m}$ of the thickness) (Figure 6). Notwithstanding this fact, corrosion activity did not increase (see discussion).

Figure 4 C_{dl} and C_{coat} trends vs the layer thickness in aerated 1N H_2SO_4 (25°C) at 1 and 168 h of immersion time

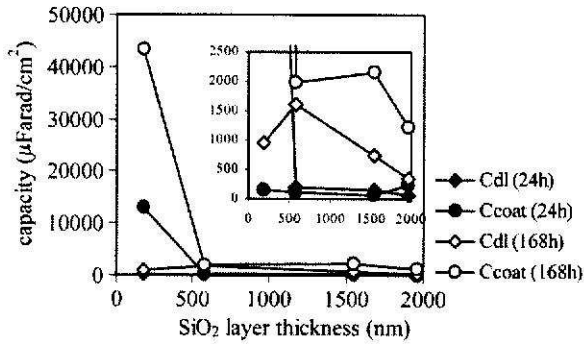


Table III The thicknesses of the PECVD treated samples obtained from the SIMS technique

Thickness (nm)	Uncertainty (per cent)	Roughness (Å)
80	40	365
80	25	270
1,550	25	280
1,950	15	190

Nano-indentation measurements

The nano-indentation measurements were performed on the surface of both uncoated and PECVD-treated brass surfaces, in order to determine their hardness. Figure 7 shows a comparison of indentation load-depth curves, carried out at the peak loads of 5 mN, on bare brass substrates and for two SiO_2 films of different thicknesses (580 and 1,950 nm).

The uncoated brass sample exhibited a smaller indentation depth and a lower amount of creep deformation during the 10 s hold period at maximum load: this implied that its hardness was higher. In addition, different samples exhibited very little variation in hardness, as evidenced by the small differences in the depth obtained at the maximum load. It was also interesting to observe the slope of the unloading segment of the load-displacement graphs and to assess the elastic recovery on unloading. For brass, the slope of the unloading

segment was almost vertical, typical of a ductile plastic material such as most metals. This indicated that the elastic strains during indentation were small compared with the plastic strains, so that most of the indenter displacement was accommodated plastically, giving little elastic recovery of the indentation depth (10 per cent). In the case of the coated samples, a larger indenter depth was recovered as the load was removed, indicating that the composite systems presented a larger degree of elastic recovery during unloading (36 per cent for the thickest). The shape of the paths related to the SiO_2 /brass systems quickly approached that of the brass substrate as the thickness of the SiO_2 coatings decreased, indicating that the surface and near-surface mechanical properties of the SiO_2 /brass system, in the examined range, depended from the coatings thickness.

Table IV reports the calculated average values of hardness for the uncoated and coated brass, together with the average values of reduced modulus and elastic recovery, determined by unloading curves for maximum peak load of 5 mN.

The substrate surface presented a hardness value in good agreement with that previously reported (Doerner and Nix, 1986) and resulted slightly harder than the SiO_2 films, whose hardness values changed only very little with the thickness. Instead, the elastic properties depended on the coating thickness and the composite systems resulted stiffer when the SiO_2 coating decreased.

In any case a remarkable improvement of the surface mechanical properties of the SiO_2 /brass system was obtained by annealing the thickest coating at 500°C in O_2 atmosphere (1 h). Figure 8 shows a comparison of indentation load-depth curves for the uncoated brass, and the SiO_2 layer (1,950 nm thick) on brass substrate as deposited and after annealing, for a single indentation carried out to peak loads of 5 mN.

The difference of the three samples is immediately clear, as evidenced by the difference of the indentation depths (obtained at the maximum load) and from the slope of the unloading segment. For the annealed sample, these data indicated, respectively, a higher hardness value and a larger degree of elastic recovery during unloading. The calculated hardness and elasticity values, reported in Table IV, indicated that the annealed sample was ~180 per cent harder and ~140 per cent stiffer than the as-deposited one. For this

Figure 5 The element profiles obtained for the 180 nm PECVD treated specimen by the SIMS technique

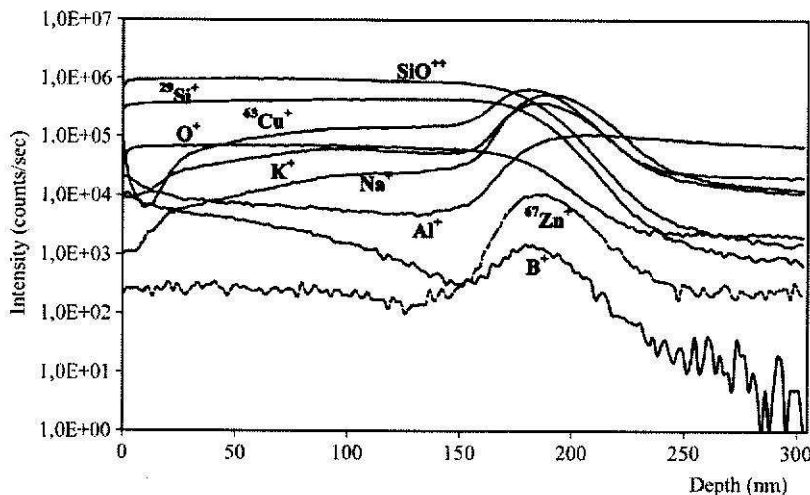


Figure 6 The element profiles obtained for the 1,950 nm PECVD treated specimen by the SIMS technique

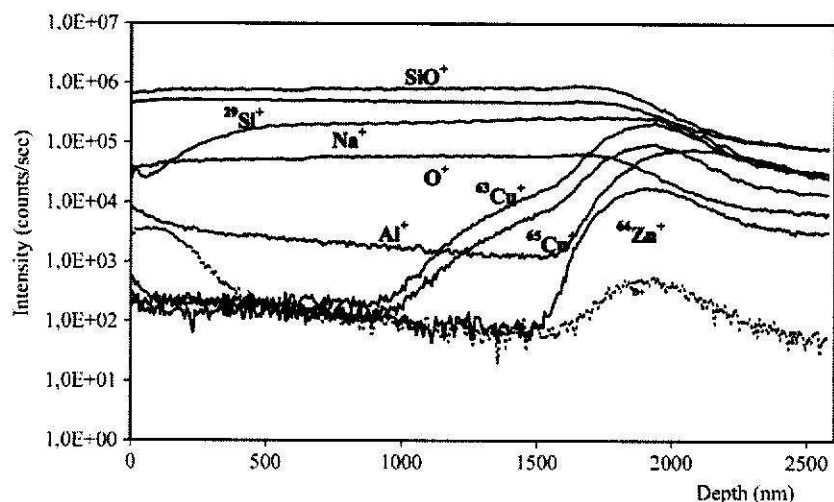


Figure 7 Load-displacement curves for: (a) uncoated brass; (b) SiO₂ coating 580 nm thick; (c) SiO₂ coating 1,950 nm thick

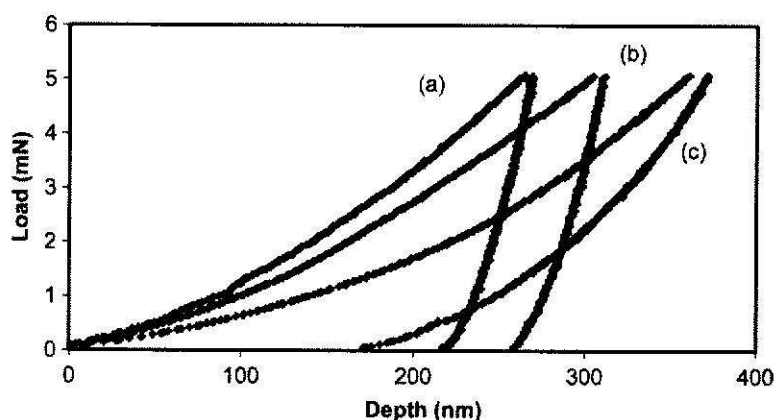


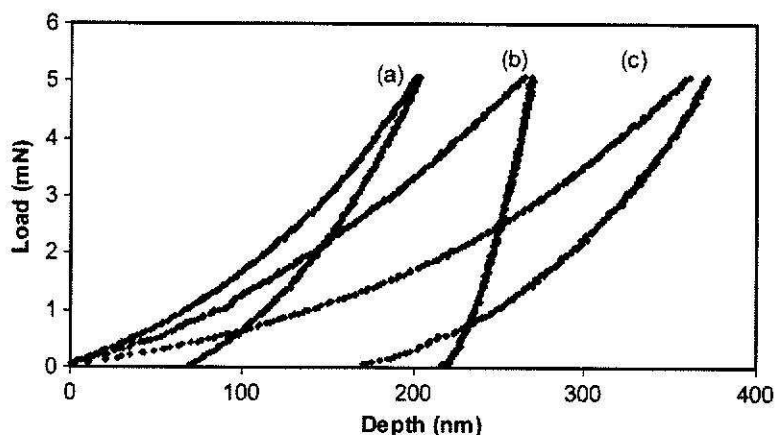
Table IV Summary of evaluated mechanical properties of SiO₂ coatings of substrate and of SiO₂/brass composite system

Sample	Hardness (GPa)	Reduced modulus (GPa)	Elastic recovery
Brass	3.03	109.46	0.10
SiO ₂ (180 nm thick)	2.49	84.91	0.08
SiO ₂ (580 nm thick)	2.34	48.96	0.17
SiO ₂ (1,550 nm thick)	2.28	27.07	0.29
SiO ₂ (1,950 nm thick)	2.53	24.46	0.36
Annealed SiO ₂ (1,950 nm thick)	7.17	57.85	0.44

situation, where a hard film covered a softer substrate, it was possible to determine the intrinsic hardness value for coating material only when the indentation depth was considerably smaller than the film thickness, since for larger indentation depths a composite hardness that also included a contribution from the substrate will be measured (Saha and Nix, 2002). This behaviour is well depicted in Figure 9, which shows the variation in hardness with depth for uncoated and annealed SiO₂ coated brass (1,950 nm thick; calculated from the indentations, covering the loading range 2.5-100 mN).

The curve of the coated sample showed a first region, at low indentation depth, where the coating hardness was almost constant, and a second region at greater indentation depths, where a decrease in the hardness – as the indentation depth increased – could be detected. This was due to a progressively increasing contribution from the substrate material, typical for a hard film on a softer substrate: the range of the hardness plateau depended on the coating thickness and the average of the values obtained in this plateau region were used to calculate the intrinsic value of the hardness of the baked SiO₂

Figure 8 Load-displacement curves for: (a) annealed SiO₂ coating 1,950 nm thick; (b) uncoated brass; (c) as-deposited SiO₂ coating 1,950 nm thick



coating (Ahn and Kwon, 2000). The average hardness result was 7.24 ± 0.10 GPa, which is in good agreement with those reported previously for as-grown PECVD SiO₂ coatings deposited on fused SiO₂ and borosilicate glass (Beck *et al.*, 1998).

Other technical tests

After the laboratory tests, the PECVD process was used to coat some industrial objects with SiO₂ anti-corrosion and anti-wear layers. Some of these objects were submitted to technical tests to determine the quality of coating achieved (e.g. exposure to the salt spray (fog) chamber test (following the ASTM B117/97 protocol). The results confirmed that the best PECVD treatment was that of the coating 1,950 nm thick, which resisted more than 800 h of salt spray fog, even at 1,550 nm thick the performance was quite good – especially from the point of view of industrial application. These industrial specimens also passed ultraviolet exposure (ASTM G53), adhesion (ASTM D3359), bending (ASTM D522), impact (ASTM 2794) and chemical (ASTM D4652) tests.

Discussion

To analyse the different thick PECVD coatings, especially when the aim is to optimise an industrial process, it is important to have the results of experimentation as soon as possible. Apart from the physical properties (for example, the

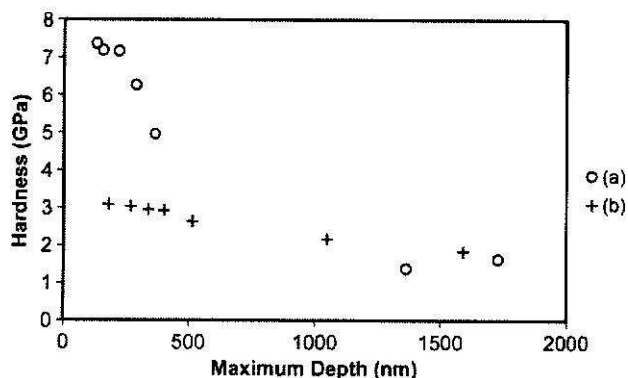
mechanical properties), the evaluation of the ability of a coating deposit to protect a metallic substrate can be usefully characterised by means of electrochemical techniques. When considering this, the differing nature of direct and alternate current techniques is complementary. Data drawn from the electrochemical techniques – “laboratory” data – can be compared with that obtained from other tests, for example, results from certain ASTM tests are important for the industrial point of view. From this comparison it is possible to have, for example, a life-time prediction of the proposed PECVD treatment.

In the present work, the same samples were examined using both in DC (Tafel curves) and in AC (EIS) to have a better vision of the whole picture. The DC technique gives an image of the entire corrosion process.

Considering the whole corrosion process, by analysing the short time test results (Figure 1), the shape of the obtained Tafel curves evidenced that both the cathodic (oxygen reduction) and the anodic (metal dissolution) part of the corrosion reaction were involved. In fact, as indicated for the anodic reaction, the anodic Tafel slope, b_A , significantly increased in the short time tests (Table I): the average b_A value obtained for the uncoated substrate was 45 mV/dec, while it increased (until 90 mV/dec for the max thickness) for the treated samples, doubling in the case of the 1,950 nm sample. This means that, at least for short immersion times, the anodic part of the corrosion reaction was greatly influenced by the PECVD treatment.

The same can be said for the cathodic part of the corrosion mechanism. While for the uncoated substrate the oxygen reduction reaction was almost unchanged – depending on the oxygen diffusion rate, due to the aerated environment, for coated specimens a different corrosion mechanism (i.e. a curve shape) was evident, see Figure 1. After 168 h, the corrosion reaction mechanism seemed to be almost the same for the various coatings, as evidenced by the curve shape that is very similar for the various specimens. As reported in Table I, the anodic Tafel slopes for the coated samples ranged all around 70 mV/dec. This could indicate, first of all, the reached homogeneity of the PECVD deposition at the various treatment time (Moretti *et al.*, 2002). The i_{corr} seemed to indicate that only the 1,550 and 1,950 nm thick coatings resisted the corrosive attack in this environment (Table I) and it was only for these samples the corrosion rates measured

Figure 9 Variation of hardness with depth for: (a) Annealed SiO₂ coating 1,950 nm thick; (b) uncoated brass substrate



after a week were one order of magnitude lower than samples with thinner coatings (about $1 \mu\text{A}/\text{cm}^2$ in comparison with about $10 \mu\text{A}/\text{cm}^2$). This finding was confirmed by the fact that it was only these specimens that appeared visually not to have sustained “damage” (i.e. not attacked from the corrosion point of view) after a week of immersion.

The E_{corr} values became as much more negative (from -113 to -174 in comparison with $-98 \text{ mV}_{\text{sce}}$ – Table I), as coating thickness increased, indicating the more cathodic behaviour of the coated samples as the layer thickness increased, compared with that of the uncoated substrate. After 24 h of immersion, all treated samples reached a similar steady-state in the corrosion reaction: this is thought to be due to the reaching of a pseudo-stationary state in the water uptake of the SiO_2 layers (Yin and Lu, 2002; Moretti *et al.*, 2002). The EIS data (see below) confirmed this conclusion. The use of EIS in evaluating the degradation, for example, of SiO_2 coatings and their interaction with aqueous environment, provides useful information that cannot be obtained with traditional DC techniques. First of all a model of equivalent circuit that represents the metal/coating behaviour in the chosen aggressive environment can be hypothesized: this allows the circuit analogy in the EIS spectra interpretation to be applied (Kendig *et al.*, 1983). EIS data analysis is often accompanied by an equivalent circuit modelling, which is an assembly of circuit elements that may represent the physical and electrical characteristics of the electrochemical interface. The equivalent circuit design, and the consequent interpretation of the EIS spectra of the coated brass, can encompass many considerations about the involved corrosion reactions, the physical properties of both coating and metal surface, and the chemical characteristics of the materials.

The physical model assumed to describe the phenomena due to the diffusion process of the reagents from the bulk solution toward the metal surface is shown in Figure 10. On the basis of this model the equivalent circuit shown in Figure 11 was chosen in accordance to the literature (Kendig and Scully, 1990). Because of the EIS is not a very

Figure 10 The physical model chosen to interpret the brass/ SiO_2 system behaviour in aerated 1N H_2SO_4 (25°C)

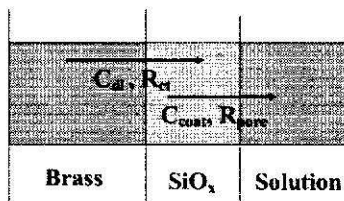
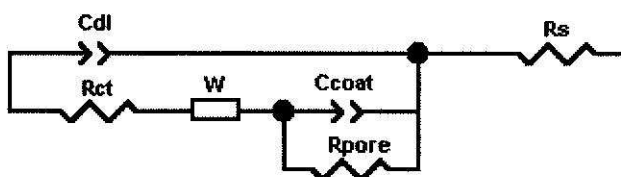


Figure 11 The equivalent circuit used to fit the EIS data of the PECVD coated specimens. C_{dl} : double-layer capacity; R_{ct} : charge-transfer resistance; W : Warburg element (diffusion parameter); C_{coat} : coating capacity; R_{pore} : pore resistance of coating; R_s : solution resistance



“perturbative” technique, the relative contributions of different electrochemical components of the circuit are easier to distinguish than is the case with dc polarisation. Further, it is possible to determine the different frequency zones at which electrochemical effects take place, and link these with the different phenomena occurring to the metal/coating and coating/solution interfaces.

The equivalent circuit proposed is formed by two parallel resistive/capacitive circuits:

- 1 The first circuit (for the high frequency part of the EIS spectrum) is characterised by the pore resistance (R_{pore}) and the coating capacity (C_{coat}) (Kendig and Scully, 1990; Mansfeld, 1993). From the electrical standpoint, the oxide layer which covers the metal surface acts as the dielectric of a condenser. The oxide film is usually represented by an RC circuit: it depicts the phenomena due to the ionic conduction through pores in the oxide film and the reactions occurring in the SiO_2 layer, which may also be influenced by the presence of the Cu ions, migrating from the substrate into SiO_2 layer. The presence of Cu ions inside the film was confirmed by the SIMS spectra (Figure 6). The presence of these ions was responsible of a very low – but significant – corrosion current in the silica coating. In series with these RC components, the W element, relates to the influence of diffusion phenomena on the system, (Lillard *et al.*, 1995).
- 2 The second circuit (for the low frequency part of the EIS spectrum) is characterised by the charge transfer resistance (R_{ct}) and the double-layer capacity (C_{dl}), taking into account the corrosion reaction (Faradic current) on a modified coated-brass surface (Bastidas *et al.*, 2000).

The non-ideal electrical behaviour takes into account constant phase elements (CPE) and the already-introduced diffusional impedance element (W) (Liu *et al.*, 2003). After short immersion times (up to 24 h) the EC may become more complicated, because, for example, part of the aggressive solution could penetrate not in a uniform way through coating pores or defects. This heterogeneous distribution of the conducting media can lead to two RC circuits in parallel, as reported by other authors (Castela and Simões, 2003).

For longer immersion times, greater than 24 h, water uptake was completed (this took, on average, at least one day of immersion): and the corrosion proceeded at pores and defects in the coating, according to the hypothesis of almost uniform electrical properties of both film and brass surface. In this way, the EIS spectrum could be simply explained.

The values reached after a week, especially for the thickest layer, indicated good anti-corrosion protection. The most significant R_{ct} value obtained at the end of the exposure period was about $14 \text{ k}\Omega \text{ cm}^2$ for the 1,950 nm specimen (168 h), which even at 48 h had already reached about $24 \text{ k}\Omega \text{ cm}^2$ (Table II).

These results appeared quite different to those obtained in the DC experiments. Furthermore, the R_{ct} value for the 1,550 nm specimens also diminished over time. This was confirmed by the R_{pore} data trend. Additionally, in this case, the EIS technique was much more useful than the conventional DC techniques, because it permits to obtain more precise information on the corrosive process to be obtained during a long term test, even if localised corrosion

degradation phenomena (for example: pitting) were not evident from visual inspection of the sample.

After 168 h of immersion, a decrease in the C_{coat} value was evident, perhaps due to the hindering of migration of the reaction products in solution that had penetrated into the film. This also meant that the water uptake was essentially complete when C_{coat} no longer varied significantly (Castela and Simões, 2003). At 1 week of exposure the minimum C_{coat} value was only reached by the 1,950 nm coating (about $1,200 \mu\text{F}/\text{cm}^2$).

Thus, a result of the electrochemical tests was that a coating 1,950 nm thick, deposited on a brass substrate, successfully resisted the onset of corrosion for at least a week of immersion in the aerated 1N H_2SO_4 . All of the other coating thicknesses exhibited lower different performances, though the 1,550 nm layer thickness achieved results that in general were comparable with those from the 1,950 coating. This was a satisfactory result as according to the findings from the salt spray fog test an industrial brass object should resist atmospheric corrosion for at least 10 years if covered by $2 \mu\text{m}$ of SiO_2 coating.

From the mechanical point of view, the silica film deposited has to maintain both its anti-corrosion and anti-wear layer performance. For this reason the same samples were subjected to the nano-mechanical test. The result was that the as-deposited SiO_2 coating on the brass substrate presented poor mechanical properties, probably due to a high residual film stress, which decreased as the coating thickness was reduced. This behaviour probably could explain the increase of the reduced modulus and the consequent decrease of the elastic recovery observed with lower thickness of silica coating, as reported in Table IV. A significant improvement of the mechanical properties of the SiO_2 coatings was obtained after annealing in oxygen atmosphere at 500°C (1 h). This treatment produced a densification process that smoothed the surface morphology (confirmed also by SEM analysis). Further experimentation and analyses are to be carried out to optimise the annealing procedure.

Conclusions

- "Laboratory" samples of brass coated by SiO_2 were tested by means of electrochemical techniques in a standard very aggressive solution (aerated 1N H_2SO_4 at 25°C) for 168 h. The surface treatment lowered the i_{corr} by almost two orders of magnitude, especially in the case of 1,550-1,950 nm coating thicknesses (1-168 h DC tests).
- AC electrochemical tests (EIS) carried out on samples in the same solution and experimental conditions showed very significant increases in R_{ct} and decreases in C_{coat} only for the samples with a 1,950 nm thick coating. Equivalent circuit modelling gave plausible interpretation of the different components of the degradation process over time (i.e. Cu migration into the SiO_2 coating during the PECVD deposition – water uptake – metal/coating interface).
- SIMS analyses, carried out on "laboratory" samples, made it possible to manage the different parameters of the deposition system and to obtain information on homogeneity and thickness (180-1,950 nm) of the coatings as well as to exclude possible defects of the layers, at least for the thicker coatings.

- Nano-indentation tests revealed large differences in the mechanical properties of as-grown and annealed SiO_2 coatings. The latter exhibited significantly higher hardness and elastic modulus, presumably due to its higher smooth surface structures. Further experimentation and analyses are to be carried out to optimise the annealing procedure for best corrosion and wear properties.

References

- Ahn, J.H. and Kwon, D. (2000), "Micromechanical estimation of composite hardness using nanoindentation technique for thin-film coated system", *Materials Science and Engineering A*, Vol. 285, p. 172.
- Amirudin, A. and Thierry, D. (1995), "Application of electrochemical impedance spectroscopy to study the degradation of polymer-coated metals", *Progress in Organic Coatings*, Vol. 26, p. 1.
- Barranco, A., Yubero, F., Cotrino, J., Espinos, J.P., Benitez, J., Rojas, T.C., Allain, J., Girardeau, T., Riviere, J.P. and Gonzales-Elipe, A.R. (2001), "Low temperature synthesis of dense SiO_2 thin films by ion beam induced chemical vapor deposition", *Thin Solids Films*, Vol. 396, pp. 9-15.
- Bastidas, J.M., Cabañes, J.M. and Catalá, R. (2000), "Corrosion behaviour of lacquered tinplate cans in contact with *Cochlides* (*Cardium edulis*) in brine solution", *Corrosion*, Vol. 56 No. 4, pp. 429-32.
- Beck, U., Smith, D.T., Reiners, G. and Dapkunas, S.J. (1998), "Mechanical properties of SiO_2 and Si_3N_4 coatings: a BAM/NIST co-operative project", *Thin Solid Films*, Vol. 332, p. 164.
- Castela, A.S. and Simões, A.M. (2003), "An impedance model for the estimation of water absorption in organic coatings. Part I: a linear dielectric mixture equation", *Corrosion Science* 45, Vol. 8, pp. 1631-46.
- Choi, J.K., Kim, D.H., Lee, J. and Yoo, Ji-B. (2000), "Effects of process parameters on the growth of thick SiO_2 using plasma enhanced chemical vapor deposition with hexamethyldisilazane", *Surface and Coating Technology*, Vol. 131, pp. 136-40.
- Doerner, M.F. and Nix, W.D. (1986), "A method for interpreting the data from depth-sensing indentation instruments", *Journal of Material Research*, Vol. 1, p. 601.
- Falcony, C., Ortiz, A., Lopez, S., Alonso, J.C. and Muhl, S. (1991), "Low temperature SiO_2 films", *Thin Solid Films*, Vol. 199, p. 269.
- Fayet, P., Holland, C., Jaccoud, B. and Roulin, A. (1995), "Commercialisation of plasma deposited barrier coatings for liquid food packaging", *Proceedings of 38th SVC Conference*, pp. 15-17.
- Growcock, B. and Jasinski, R.J. (1989), "Time-resolved AC impedance spectroscopy of mild steel in concentrated hydrochloric acid", *Journal of Electrochemical Society*, Vol. 136, p. 2310.
- Inagaki, N., Kondo, S., Hirata, M. and Urushibata, H. (1989), "Plasma polymerization of organosilicon compounds", *Journal of Applied Polymer Science*, Vol. 30, p. 3385.
- Jüttner, K., Lorenz, W.J., Kendig, M.W. and Mansfeld, F. (1988), "Electrochemical impedance spectroscopy on 3-d inhomogeneous surfaces, corrosion in neutral aerated solutions", *Journal of Electrochemical Society*, Vol. 135, p. 332.

- Kendig, M. and Scully, J. (1990), "Basic aspects of electrochemical impedance application for the life prediction of organic coatings on metals", *Corrosion*, Vol. 46, p. 22.
- Kendig, M., Mansfeld, F. and Tsai, S. (1983), "Determination of the long term corrosion behaviour of coated steel with A.C. impedance measurements", *Corrosion Science*, Vol. 23 No. 4, pp. 317-29.
- Kittel, J., Celati, N., Keddam, M. and Takenouti, H. (2002), "New insight into the corrosion protection by organic coatings and the evaluation of degradation by EIS", *Proceedings of the 15th International Corrosion Congress*, Granada, 22-27 September, Paper no. 511, p. 335.
- Lillard, R.S., Kruger, J., Tait, W.S. and Moran, P.J. (1995), "Using local electrochemical impedance spectroscopy to examine coating failure", *Corrosion Science*, Vol. 51 No. 4, pp. 251-9.
- Liu, C., Bi, Q., Leyland, A. and Matthews, A. (2003), "An electrochemical impedance spectroscopy study of the corrosion behaviour of PVD coated steels in 0.5 N NaCl aqueous solution: Part I: establishment of equivalent circuits for EIS data modelling", *Corrosion Science*, Vol. 45, pp. 1243-56.
- Mansfeld, F. (1993), "Models for the impedance behaviour of protective coatings and cases of localized corrosion", *Electrochimica Acta*, Vol. 38, p. 1891.
- Moretti, G., Guidi, F., Canton, R., Capobianco, G., Glisenti, A. and Battagliarin, M. (2002), "An industrial PECVD application: modified SiO₂ films deposited on OT59 brass for wear and corrosion protection", *Proceedings of the 15th International Corrosion Congress*, Granada, 22-27 September, Paper no 582, p. 208.
- Okuara, J.M. and White, A. (1987), "Preparation of SiO₂ overlayers on oxide substrates by chemical vapor deposition of Si(OC₂H₅)₄", *Applied Surface Science*, Vol. 29, p. 223.
- Oliver, W.C. and Pharr, G.M. (1992), "An improved technique for determining hardness and elastic modulus using load and displacement sensing indentation experiments", *Journal of Materials Research*, Vol. 7 No. 6, p. 1564.
- Pagura, C., Daolio, S. and Facchin, B. (1992) in Benninghoven, A., Jansen, K.T.F., Tumpner, J. and Werner, H.W. (Eds), *Secondary Ion Mass Spectrometry SIMS VIII*, Wiley, Chichester, p. 239.
- Patrick, W.J., Schwartz, G.C., Cahpple-Sokol, J.D., Carruthers, R. and Olsen, K. (1992), "Plasma-enhanced chemical vapor deposition of silicon dioxide films using tetraethoxysilane and oxygen: characterization and properties of films", *Journal of Electrochemical Society*, Vol. 139, p. 2604.
- Perrin, J., Schmitt, J., Hollenstein, Ch., Howling, A.A. and Sansonnens, L. (2000), "The physics of plasma-enhanced CVD for large area coating: industrial application to flat panel display and solar cells", *Plasma Phys. & Contr. Fusion*, Vol. 42 No. 12B, pp. 353-63.
- Popov, B.N., Alwohaibi, S. and White, R.E. (1993), "Using electrochemical impedance spectroscopy as a tool for organic coating solute saturation monitoring", *Journal of Electrochemical Society*, Vol. 140 No. 4, pp. 947-51.
- Rats, D., Hajek, V. and Martinu, L. (1999), "Micro-scratch analysis and mechanical properties of plasma-deposited silicon-based coatings on polymer substrates", *Thin Solid Films*, Vol. 340, p. 33.
- Saha, R. and Nix, W.D. (2002), "Effects of the substrate on the determination of thin film mechanical properties by nanoindentation", *Acta Materialia*, Vol. 50, p. 23.
- Sahli, S., Segui, Y., Hadj Moussa, S. and Djouadi, M.A. (1992), "Growth, composition and structure of plasma-deposited siloxane and silazane", *Thin Solid Films*, Vol. 217, pp. 17-25.
- Sahli, S., Segui, Y., Ramdani, S. and Takkouk, Z. (1994), "R.F. plasma deposition from hexamethyldisiloxane-oxygen mixtures", *Thin Solid Films*, Vol. 250, pp. 206-12.
- Santagata, D.M., Sere, P.R., Elsner, C.I. and Di Sarli, A.R. (1998), "Evaluation of the surface treatment effect on the corrosion performance of paint coated carbon steel", *Progress in Organic Coatings*, Vol. 33, p. 44.
- Schreiber, H.P., Wertheimer, M.R. and Wrobel, A.M. (1980), "Corrosion protection by plasma-polymerized coatings", *Thin Solids Films*, Vol. 72, p. 487.
- Selamoglou, N., Mucha, J.A., Ibbotson, D.A. and Flamm, D.L. (1989), "Silicon oxide deposition from tetraethoxysilane in a radiofrequency downstream reactor: mechanisms and step coverage", *Journal of Vacuum Science and Technology*, Vol. B7, p. 1345.
- Tien, P., Smolinsky, G. and Martin, R. (1972), "Thin organosilicon films for integrated optics", *Applied Optics*, Vol. 11, p. 637.
- van Ooij, W.J., Sabata, A., Zeick, D.B. and Connors, K.D. (1995), "Metals-surface preparation by plasma-polymerized films", *Journal of the Electrochemical Society*, Vol. 95-13, p. 299.
- Walter, G.W. (1991), "The application of impedance spectroscopy to study the uptake of sodium chloride solution in painted metals", *Corrosion Science*, Vol. 32, p. 1041.
- Yasuda, H.K. (1987), "Plasma polymerization & plasma treatment: journal of applied polymer science", John Wiley & Sons, Polymer Science, Applied Polymer Symposium 38/42, New York, NY, p. 357.
- Yin, K.M. and Lu, L.I. (2002), "Impedance analysis of organic coating in hydrochloric acid solutions", *Proceedings of 15th International Corrosion Congress*, Granada, 22-27 September, Paper no. 240, p. 334.